Far infrared photonic crystals operating in the Reststrahl region

Richard A. Soref[1*], Zexuan Qiang[2] and Weidong Zhou[2*]

[1]*Sensors Directorate, Air Force Research Laboratory, AFRL/SNHC, Hanscom Air Force Base, MA 01731-2909*
[2]*Department of Electrical Engineering, NanoFAB Center, University of Texas at Arlington, Arlington, TX 7601-*
**Corresponding authors: Richard.Soref@hanscom.af.mil; wzhou@uta.edu*

Abstract: We report here far infrared photonic crystals comprised of a lattice-matched pair of semiconductor materials: GaP and Si, or GaAs and Ge, or AlAs and GaAs. The crystals operate in a wavelength range where the real refractive index of one material undergoes a major dispersion associated with the LO and TO phonon absorption peaks. Using electromagnetic theory, we investigated the photonic-bandgap response for both TE and TM polarizations. Propagation losses for two types of crystals are estimated in this paper. These structures offer promise for the integration of III-V materials (GaP, GaAs) on group IV (Si, or Ge) for practical, active, far infrared photonic devices, such as light sources, amplifiers, modulators, reconfigurable waveguides and switches.

OCIS codes: (230.0230) Optical devices; (130.3130) Integrated optics materials; (230.7390) Waveguides; (999.9999) Photonic crystals

References and links

1. E. Yablonovitch, "Photonic band-gap crystals," J. Phys. **5**, 2443-2460 (1993).
2. M. Tokushima, H. Yamada, and Y. Arakawa, "1.5um-wavelength light guiding in waveguides in square-lattice-of-rod photonic crystal slab," Appl. Phys. Lett. **84**, 4298-4300 (2004).
3. W. D. Zhou, "Encapsulation for efficient electrical injection of photonic crystal surface emitting lasers," Appl. Phys. Lett. **88,** 051106 (2006).
4. W. Zhou, V. Nair, and G. Thiruvengadam, "The impact of high dielectric constant on photonic bandgaps in PbSe nanocrystal-based photonic crystal slabs," Proc. SPIE **6128**, 61280B (2006).
5. E. D. Palik, *Handbook of Optical Constants of Solids*, (Academic Press, 1985) Vol. I.
6. M. Wakaki, K. Kudo, and T. Shibuya, *Physical Properties and Data of Optical Materials* (CRC Press, 2007).
7. M. Plihal and A. A. Maradudin, "Photonic band structure of two-dimensional systems: The triangular lattice," Phys. Rev. B **44**, 8565-8571 (1991).
8. R. Leiten, "Germanium-a surprise base for high-quality nitrides," Compd. Semicond. **13**, 14-17 (2007).
9. C. G. Ribbing, "Reststrahlen material bilayers- An option for tailoring in the infrared," Appl. Opt. **32**, 5531-5534 (1993).
10. J. A. Dobrowolski, Y. Guo, T. Tiwald, P. Ma, and D. Poitras, "Toward perfect antireflection coatings. 3. Experimental results obtained with the use of Reststrahlen materials," Appl. Opt. **45**, 1555-1562 (2006).
11. A. Rung and C. G. Ribbing, "Polaritonic and Photonic Gap Interactions in a Two-Dimensional Photonic Crystal," Phys. Rev. Lett. **92**, 123901 (2004).
12. A. Rung, C. G. Ribbing, and M. Qiu, "Gap maps for triangular photonic crystals with a dispersive and absorbing component," Phys. Rev. B **72**, 205120 (2005).
13. M. M. Sigalas, C. M. Soukoulis, C. T. Chan, and K. M. Ho, "Electromagnetic-wave propagation through dispersive and absorptive photonic-band-gap materials," Phys. Rev. B **49**, 11080 (1994).
14. V. Kuzmiak and A. A. Maradudin, "Photonic band structures of one- and two-dimensional periodic systems with metallic components in the presence of dissipation," Phys. Rev. B **55**, 7427 (1997).
15. A. Taflove and S. C. Hagness, *Computational Electrodynamics: The Finite-difference Time-domain Method* (Artech House, 2000).
16. J. B. Pendry, "Photonic Band Structures," J. Mod. Opt. **41**, 209-229 (1994).
17. G. Veronis, R. W. Dutton, and S. Fan, "Metallic photonic crystals with strong broadband absorption at optical frequencies over wide angular range," J. Appl. Phys. **97**, 093104 (2005).

#84558 - $15.00 USD Received 26 Jun 2007; revised 2 Aug 2007; accepted 3 Aug 2007; published 8 Aug 2007

18. M. Qiu and S. He, "A nonorthogonal finite-difference time-domain method for computing the band structure of a two-dimensional photonic crystal with dielectric and metallic inclusions," J. Appl. Phys. **87**, 8268 (2000).
19. E. D. Palik, *Handbook of Optical Constants of Solids*, (Academic Press, 1991) Vol. II.
20. J. D. Joannopoulos, R. D. Meade, and J. N. Winn, *Photonic Crystals* (Princeton University Press, Princeton, 1995).

1. Introduction

Today, most two-dimensional photonic crystals consist of a dielectric slab that is perforated by a periodic 2D array of columnar air holes [1]. To give high index contrast, the holes are usually filled with air or low index materials (e.g. oxide, polymer, or nanoparticles) [2-4]. In this paper, we propose that useful photonic crystals (PhCs) can be constructed from two intrinsic, lattice-matched semiconductors A and B, such that semiconductor B is grown selectively within the holes of slab A. This A/B slab can then be clad above and below by air, for example, giving high index contrast in the vertical direction. In the horizontal plane, the index contrast between A and B can also be large, as described in this paper. The integration of III-V semiconductor materials (such as GaAs, GaP) with group IV materials (such as Si, Ge) offer promise for practical active far infrared photonics, such as light sources, amplifiers, modulators, reconfigurable waveguides and switches.

If we examine the longwave absorption spectra of the polar-bonded III-V semiconductors, we find that there are significant absorption peaks in the far infrared that are associated with LO and TO phonons. This spectral regime is known as the Reststrahl region. In the III-V, the wavelength of infrared-light resonance with the transverse- and longitudinal- optic lattice-vibration wavelength is 27.24 μm for TO in GaP, 24.81 μm for LO in GaP, 37.17 μm for TO in GaAs and 34.25 μm for LO in GaAs [5, 6]. The very strong phonon-induced absorption peak of the III-V semiconductor in the Reststrahl region is due primarily to the fundamental TO phonon, and there is a weak LO phonon absorption at the shorter wavelength. The reason for the TO dominance is that the optical electric field of the infrared beam oscillates transverse to the beam propagation direction, and this transverse direction coincides with the direction of transverse ion motion in the polar-bonded III-V.

The polariton-induced absorption α is linked to the optical extinction coefficient k by the relation $\alpha = 4\pi k/\lambda$, where k is the imaginary part of the complex refractive index ($\tilde{n} = n + ik$), n is the real part of $\tilde{n}$, and λ is the free-space wavelength. The spectrum of the imaginary part k is linked to the spectrum of the real part n by the Kramers-Kronig relations. Thus, as is well known, there is considerable dispersion of the real index in the Reststrahl region (R-region), where the n-spectrum looks like the derivative of the peaked k-spectrum.

In this paper, we propose and investigate far infrared photonic crystals comprised of two types of semiconductor materials in which the index of one semiconductor is anomalously low or high due to phonon-induced dispersion. Our research has shown that there are actually two types of 2D PhCs. Type 1 has the high-to-low index approach and type 2, the reverse. Fig. 1 illustrates the geometry. In type 1 PhCs, the slab index is higher than the hole-filling-material's index; whereas, type 2 PhCs have a slab index that is lower than the hole index. Type 2 is counter-intuitive but is quite viable, as shown by electromagnetic theory [7]. The advantage of operating in the R-region is the high index contrast that is offered for types 1 and 2. The disadvantage is the high propagation loss, an infrared attenuation that will in practice limit the 2D PhC network length to several hundred micrometers. We have made estimates of R-related loss in this paper. We consider only circular columns in this paper, though the columns can be of any arbitrary shapes.

The focus in this paper is on lattice-matched pairs of undoped crystalline semiconductors, namely Ge and GaAs; and Si and GaP. We did not investigate other matched pairs such as cubic InGaN and GaAs or the recent pairing [8] of GaN with Ge in which hexagonal GaN is grown 5:4 on (111) Ge. The A/B concept can also be extended to semiconductor/non-

#84558 - $15.00 USD Received 26 Jun 2007; revised 2 Aug 2007; accepted 3 Aug 2007; published 8 Aug 2007

semiconductor PhCs that employ the phonon-associated dispersion of amorphous Beryllium oxide (BeO), SiO_2 and GeO_2 in the long-wave infrared region [9-11].

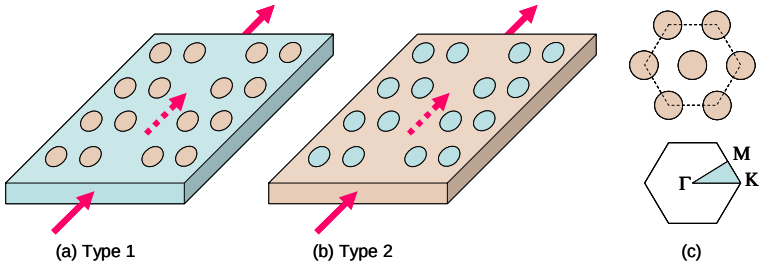

Fig. 1. Schematic of proposed (a) type 1 and (b) type 2 photonic crystals consisting of two types of semiconductor materials; (c) the hexagonal lattice and the corresponding first Brillouin zone with the high symmetry points Γ, M and K.

In fact, photonic bandgap properties were reported by Rung *et al.* [12] on ceramic BeO material systems operating in the Reststrahl region for infrared applications, where both photonic bandgaps and polaritonic gaps were observed. The simulation of these material systems with strong dispersive and absorptive properties is quite difficult [12]. Different approaches have been reported, including the transfer matrix method (TMM) [13], the plane wave expansion (PWE) technique [14] and the finite-difference time-domain (FDTD) technique [12,15]. The dielectric function can be modeled with either the Drude model for metals [14,16,17] or the Lorentz model for semiconductors [12,18]. However, when using the FDTD technique to get the bandgap, care should be taken to determine the peaks of the spectral distribution by Fourier transform, which correspond to the locations of the *eigen* frequencies. It is thus very time consuming to get different gap maps for different parameters.

In this paper, we first consider an ideal scenario, that is, non-absorptive and non-dispersive material, to explore some possible spectral windows by using the plane-wave expansion method (PWE) in two-dimensional structures. The bandgaps obtained here will be different from the real gaps, as the real gaps require a full *three-dimensional* photonic crystal slab simulation, taking into account the dispersion and absorption effects. Nevertheless, our approach offers design guidelines in terms of the structural parameters, such as the index differences and the circular column radius as compared to the lattice constant. The bandgaps for types 1 and 2 PhCs for both TE and TM polarizations were calculated and we obtain wavelength regions over which the bandgap exists (denoted as "window 1" and "window 2").

Later we consider the effect of a real scenario with strongly dispersive and absorptive properties by using the frequency-dependent FDTD at the corresponding window, to obtain the propagation losses of line-defect photonic crystal waveguide (one line of columns are removed). At "window 2", the propagation loss is smaller, which corresponds to the so-called polaritonic bandgap [12,13].

2. Experimental n and k data on lattice-matched semiconductors

The experimental results on n and k from the literature have been compiled in two Handbooks edited by Palik [5,19]. We have plotted this data as a function of wavelength for GaAs and Ge (Fig. 2, GaP and Si (Fig. 3). The n and k indices for A and B, the index difference Δn between A and B, and the propagation loss in materials A and B are plotted. The loss in dB/cm is given by L = 4.34α where the absorption coefficient α [cm^{-1}] is $4\pi k/\lambda$. It is worth mentioning that the complex frequency-dependent dielectric function expression ($\tilde{\varepsilon} = \varepsilon_1 + i\varepsilon_2$) can relate to the complex refractive index expression ($\tilde{n} = n + ik$) with $\varepsilon_1 = n^2 - k^2$, and $\varepsilon_2 = 2nk$. The complex refractive index expression is used here for better presentation of the bandgap plots and propagation loss analysis.

#84558 - $15.00 USD Received 26 Jun 2007; revised 2 Aug 2007; accepted 3 Aug 2007; published 8 Aug 2007

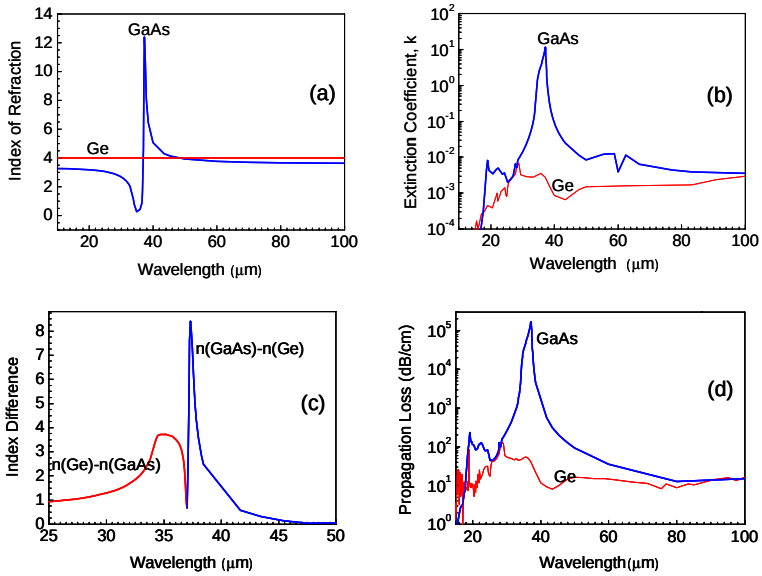

Fig. 2. Index of GaAs and Ge in the long wave and far-infrared spectral regime: (a) real part of index, (b) imaginary part of index, (c) refractive index difference between GaAs and Ge, and (d) the propagation loss of GaAs and Ge.

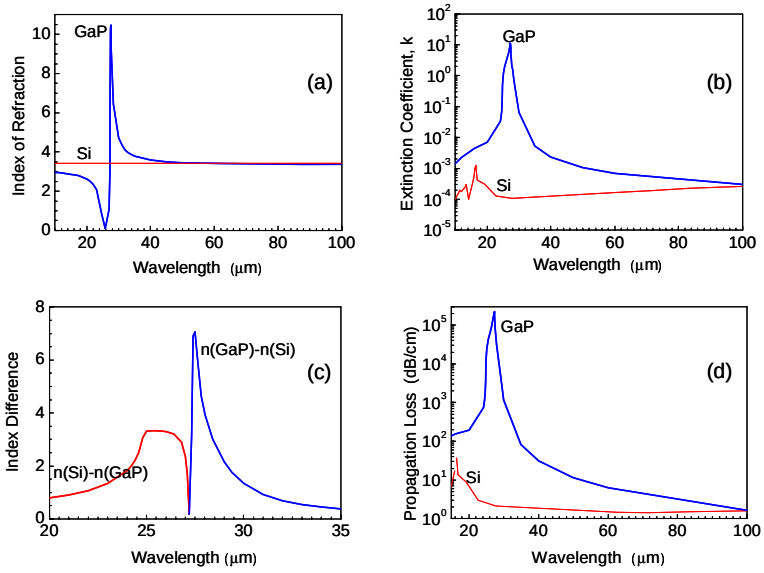

Fig. 3. Index of GaP and Si in the long wave and far-infrared spectral regime: (a) real part of index, (b) imaginary part of index, (c) refractive index difference between GaP and Si, and (d) propagation loss of GaP and Si.

3. The photonic bandgaps

For all 2D simulations in this paper, a hexagonal lattice of circular columnar holes is assumed. The center-to-center spacing of holes (lattice parameter) is a, and the hole radius is r. We first made momentum-space plots of the PhC band structure by picking trial values of

#84558 - $15.00 USD Received 26 Jun 2007; revised 2 Aug 2007; accepted 3 Aug 2007; published 8 Aug 2007

Δn, r, and a/λ, assuming k = 0 for both A and B. The result was that a bandgap in the bandstructure existed if and only if the index difference Δn was about 1.5 or greater. Knowing this, we then defined two spectral windows in the Reststrahl region for further study. We have labeled these as Window 1 and Window 2 in Fig. 4(a) and 4(b) where Δn < -1.5 and Δn > 1.5 for W1 and W2, respectively. The corresponding LO and TO wavelengths are indicated in the plots for GaAs and GaP, respectively. Also labeled are the wavelengths *a,b,c,d,e,f* at which the PhC propagation loss can be estimated. The bandgap for these two window regions are investigated with examples given in the following sections.

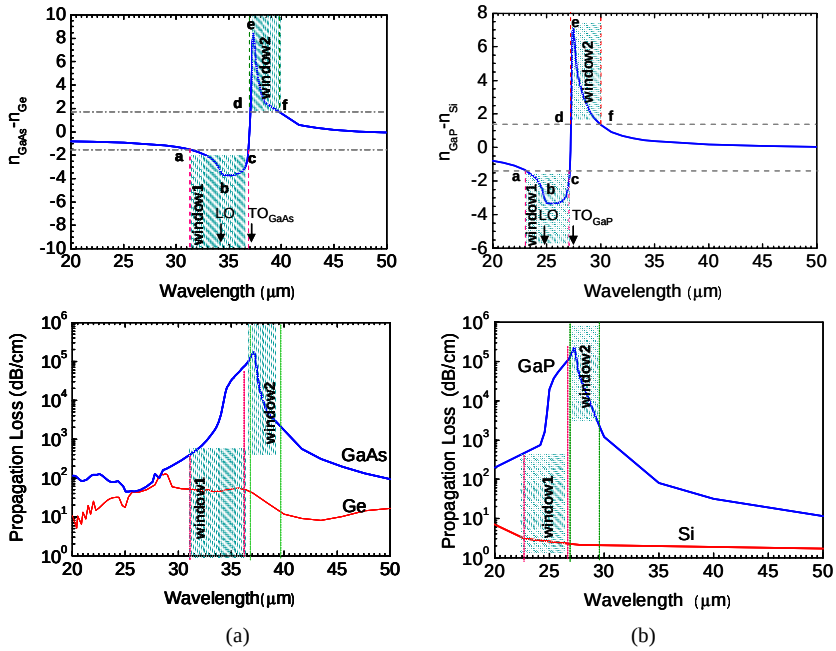

Fig. 4. (a). Index difference between GaAs and Ge, and absorption of GaAs and Ge in the spectral windows 1 and 2 that are situated within the GaAs Reststrahl-dispersion region; (b). Index difference between GaP and Si, and absorption of GaP and Si in the spectral windows 1 and 2 that are situated within the GaP Reststrahl-dispersion region.

3.1 Crystals in the high index portion ("Window 2")

From the above figures, we have selected several key examples for modeling to reveal the PhC behavior: These are GaAs/Ge and GaP/Si systems at a wavelength for which the index contrast is high, as follows (corresponding to the "Window 2" regions in Fig. 4). At λ = 37.52 μm, the GaAs and Ge indices are 10.6 and 3.989, respectively. At λ = 27.80 μm, the GaP and Si indices are 8.06 and 3.42, respectively. In practice, the slab of semiconductor A would be bounded above and below by air, as in a suspended "membrane". However, our numerical simulation approach is "true 2D" and does not take into account this 3D cladding situation. Nevertheless, we believe that the 2D results will give a strong indication of the 3D behavior.

Our first simulation was to scan r/a for a photonic bandgap, and here we take k = 0 for both materials. Starting with Ge posts within the GaAs slab (type 1), we found, after scanning trials (Fig. 5(a)), that a definite bandgap exists for the TE polarization. The bandgap dispersion plots are illustrated in Fig. 5(c), for r/a = 0.4. This gap is present over the wavelength range from 31.65 μm to 45.5 μm with a = 3.64 μm. Scanning next for the TM gap, we find, as shown in Fig. 5(b) and 5(d), a bandgap that exists from 36.68 μm to 38.43 μm when r/a = 0.4 and a = 8.07 μm. Turning next to type 2, the GaAs posts within the Ge slab (Fig. 6), we find the TE gap is present in the wavelength range from 36.00 to 39.13 μm

#84558 - $15.00 USD Received 26 Jun 2007; revised 2 Aug 2007; accepted 3 Aug 2007; published 8 Aug 2007

when r/a = 0.2 and a = 9.00 μm. Also in this type 2, the TM gap is found from 32.16 μm to 48.00 μm when r/a = 0.2 and a = 4.12 μm.

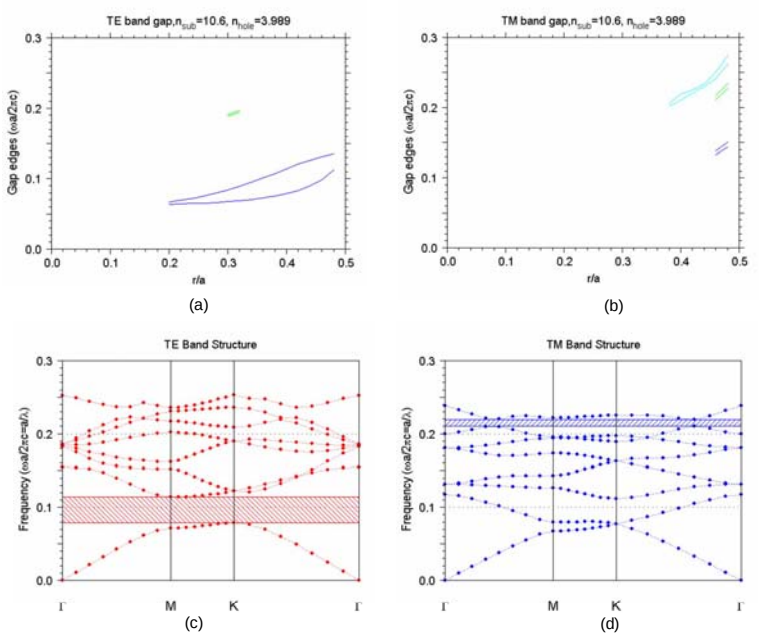

Fig. 5. Photonic bandgap for Type 1 photonic crystals (Ge column in GaAs slab): Gap maps at different r/a values for (a) TE and (b) TM polarizations; Bandgap plots at r/a=0.4 for (c) TE and (b) TM polarizations.

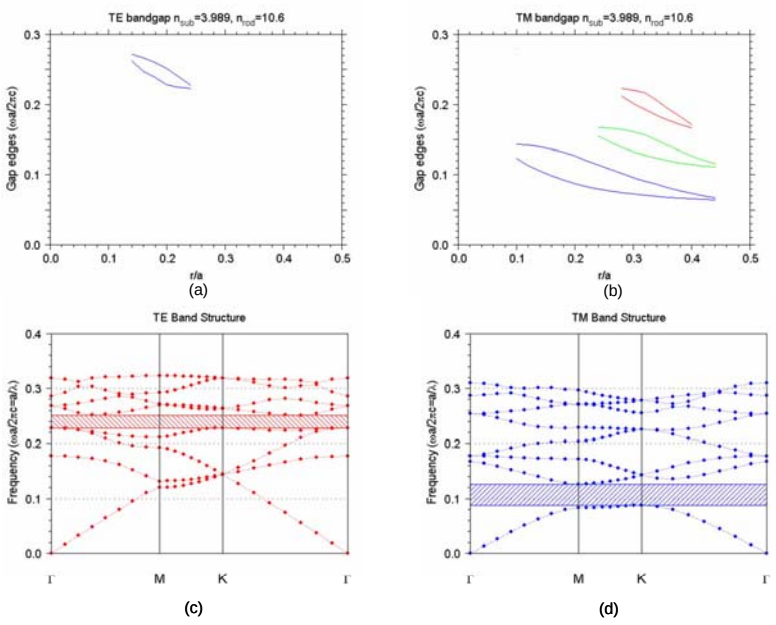

Fig. 6 Photonic bandgap for Type 2 photonic crystals (GaAs column in Ge slab): Gap maps at different r/a values for (a) TE and (b) TM polarizations; Bandgap plots at r/a=0.2 for (c) TE and (b) TM polarizations.

#84558 - $15.00 USD Received 26 Jun 2007; revised 2 Aug 2007; accepted 3 Aug 2007; published 8 Aug 2007

Going next to the type 1 crystal of Si columns within the GaP slab, we obtain a TE bandgap, shown in Fig. 7, over 23.79 μm to 33.30 μm for r/a = 0.4 and a = 3.33 μm. Here, the TM gap of Fig. 7 exists from 27.71 μm to 27.9 μm (quite narrow) when r/a = 0.4 and a = 7.65 μm. Proceeding to the type 2 PhC with GaP columns inside a Si slab (Fig. 8), we determine a TE gap from 26.87 μm to 28.79 μm (quite narrow) for r/a = 0.2 and a = 8.06 μm, while the TM gap is present from 24.19 μm to 34.10 μm when r/a = 0.2 and a = 3.75 μm.

Generally, TE is preferred for type 1 (air-hole-like) and TM preferred for type 2 (dielectric-rod-like) [20]. The AlAs/GaAs gap results, not presented here, are similar in outline to those of GaAs/Ge and GaP/Si.

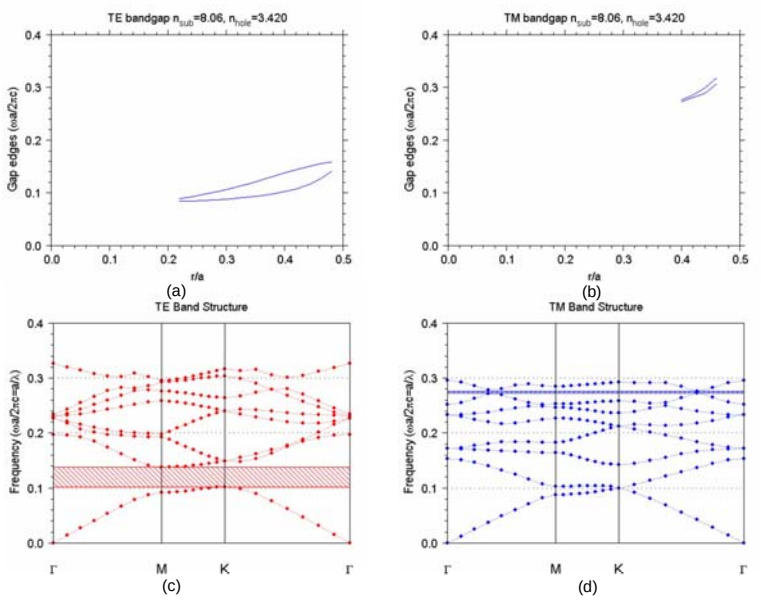

Fig. 7. Photonic bandgap for Type 1 photonic crystals (Si column in GaP slab): Gap maps at different r/a values for (a) TE and (b) TM polarizations; Bandgap plots at r/a=0.4 for (c) TE and (b) TM polarizations.

3.2 Crystals in the low index portion ("Window 1")

On the short-wavelength side of the polariton-peaks, the III-V index n dips down before rising up sharply (corresponding to the "Window 1" regions in Fig. 4). This dip region is useful for creating a type-1 PhC in which the A/B index contrast is fairly high. Because the index contrast is equally high in the type 2 geometry, we wanted to confirm the existence of type-2 PhCs in this spectral region. We found bandgaps for some instances of TE- polarized infrared propagation in the slab, and gaps for some cases of TM. When investigating the gaps, k = 0 was at first assumed for both A and B. Then, when actual k values were introduced, the gap changed by only a few percent. Some representative k = 0 results that were obtained near point *a* in Figs 5 and 6 are presented in Fig. 9 where the frequency $\omega a/2\pi c$ of the upper and lower gap edges is plotted as function of r/a. Multiple gaps are found in some cases. The gap-map examples in Fig. 9 refer to λ = 34.50 μm where n (GaAs) = 0.76 and n(Ge) = 3.99, and to λ = 25.58 μm where n(GaP) = 0.36 and n(Si) = 3.42. We see in Fig. 9 that photonic bandgaps are present in both type 1 and type 2 PhCs, thus supporting the fundamental proposition of this paper. The AlAs/GaAs gap results, not presented here, are similar in outline to those of GaAs/Ge and GaP/Si.

#84558 - $15.00 USD Received 26 Jun 2007; revised 2 Aug 2007; accepted 3 Aug 2007; published 8 Aug 2007

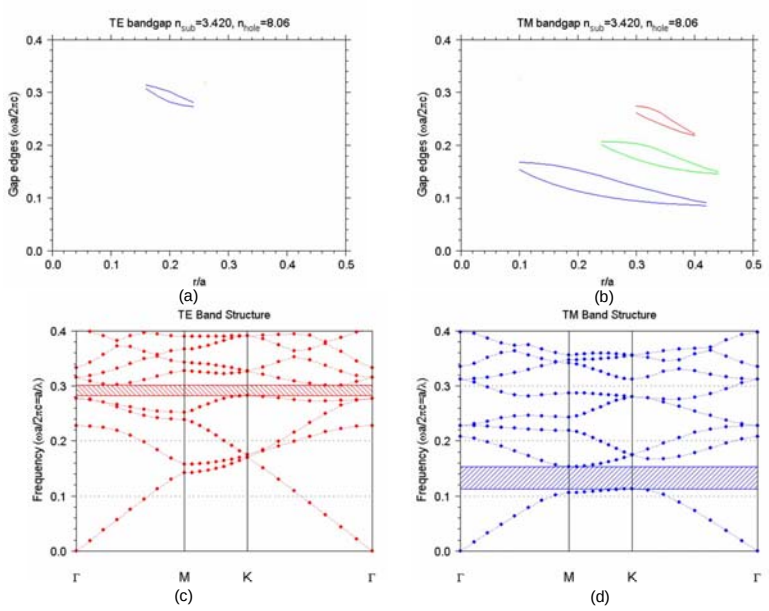

Fig. 8. Photonic bandgap for Type 2 photonic crystals (GaP column in Si slab): Gap maps at different r/a values for (a) TE and (b) TM polarizations; Bandgap plots at r/a=0.2 for (c) TE and (b) TM polarizations.

4. Photonic-crystal waveguide loss due to phonon absorptions

Since the absorption (k-values) are quite large within the Reststrahl band, it is important to determine whether this attenuation has a serious effect upon the PhCs. We therefore investigated how strongly the infrared light is attenuated in a line-defect waveguide. 2D frequency-dependent FDTD with a perfectly-matched layer (PML) boundary was used to track the amplitude of far infrared launched into the single line-defect waveguides as shown in Fig. 10. A photodetector was placed at the output of a waveguide whose length L was 40a in order to determine the output spectrum's amplitude for a flat-spectrum input at specific wavelengths shown in Table 1 and Table 2 for different cases. The propagation loss (PL) can be derived from the output power P_B and the incident power P_A based on the equation: $PL = -10\log_{10}(P_B / P_A)/L$. We examined ten particular cases for the GaP and Si system, and ten cases for GaAs and Ge. For each case, two simulation runs were carried out to get the results for the structure without and with absorption, as shown in Fig. 11, for the case shown in Table 1 for type 2 GaP/Si(2.0/3.42) case with wavelength of 23.06μm and r/a=0.4. The results are summarized in Table 1 and Table 2 where the waveguide propagation loss using the actual k values are given in the last two columns. It is worth mentioning that care should be taken when simulating the structure with real index less than 1.0, and with CW source input. The grid resolution should be no larger than λ/10, where λ is the shortest wavelength of interest in the material with highest real part of the index. The time step has to be further reduced to ensure stable simulation runs. For strongly dispersive and absorptive material, it is highly desirable to use large simulation time.

Here are the key findings of Table 1 and Table 2. Photonic bandgaps are found in both type 1 and type 2 photonic crystals within both the low-and-high index dispersion regions (Windows 1 and 2)—confirming our thesis. Also, the propagation losses of line-defect waveguides in type 1 PhCs are higher, or much higher, than the losses in type 2 PhC waveguides, a result found in windows 1 and 2. Because the type 1 losses range from 786 to 6676 dB/cm, we judge the type 1 PhC devices to be impractical.

#84558 - $15.00 USD Received 26 Jun 2007; revised 2 Aug 2007; accepted 3 Aug 2007; published 8 Aug 2007

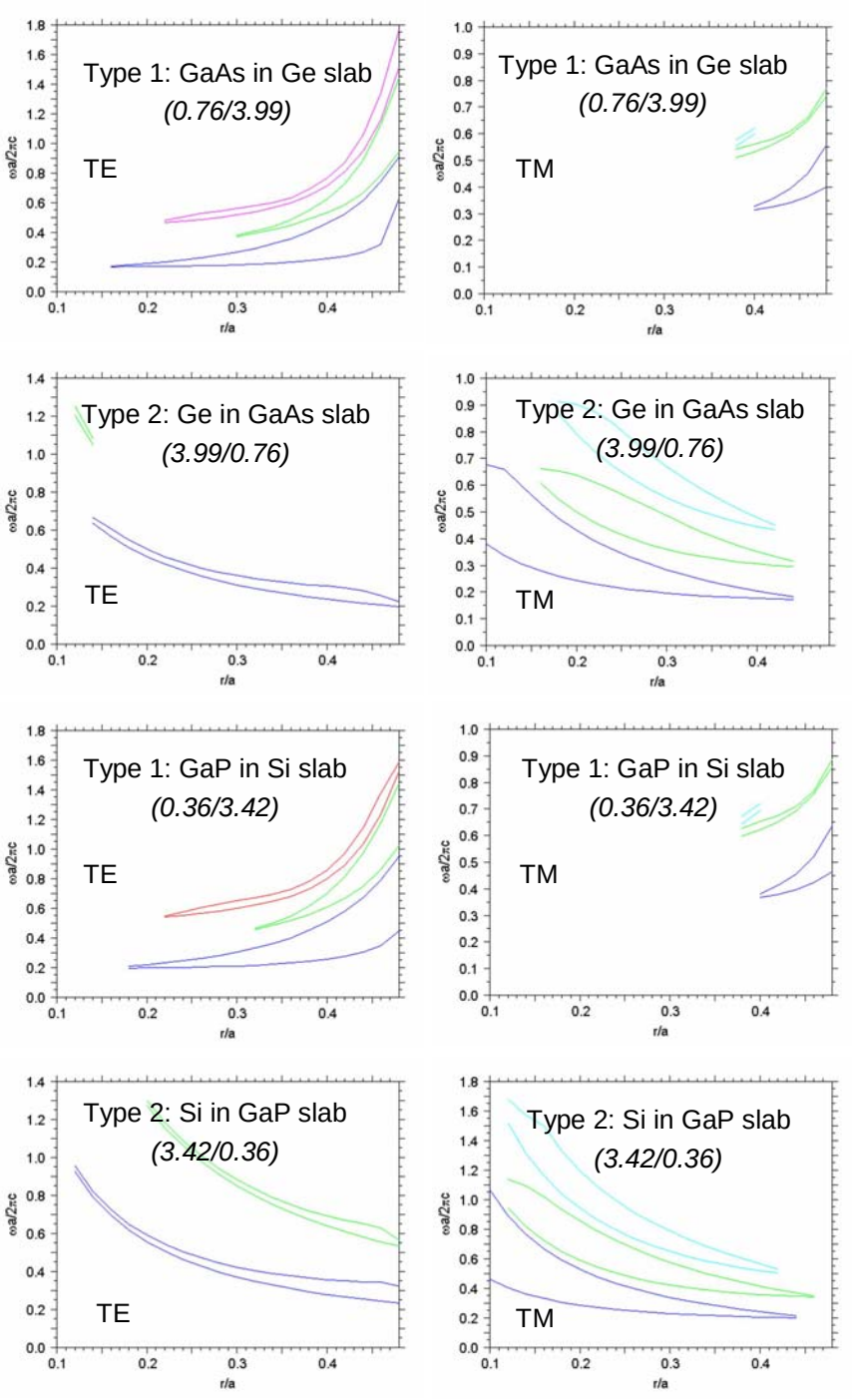

Fig. 9. Bandgap maps of photonic crystals in the low-index portion of the dispersion region: Ge/GaAs at $\lambda = 34.50$ μm and Si/GaP at $\lambda = 25.58$ μm.

#84558 - $15.00 USD Received 26 Jun 2007; revised 2 Aug 2007; accepted 3 Aug 2007; published 8 Aug 2007

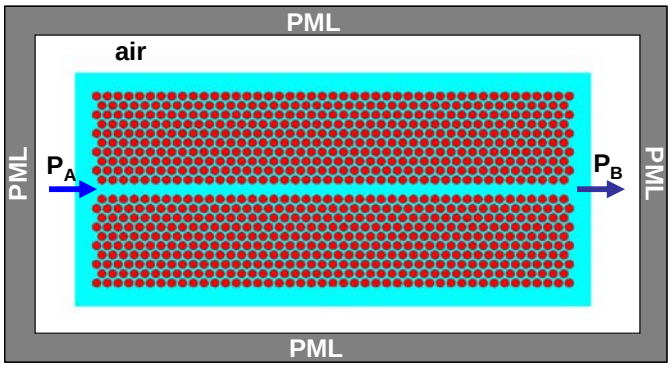

Fig. 10. Schematic of the simulation setup used for the propagation loss analysis associated with the material absorption.

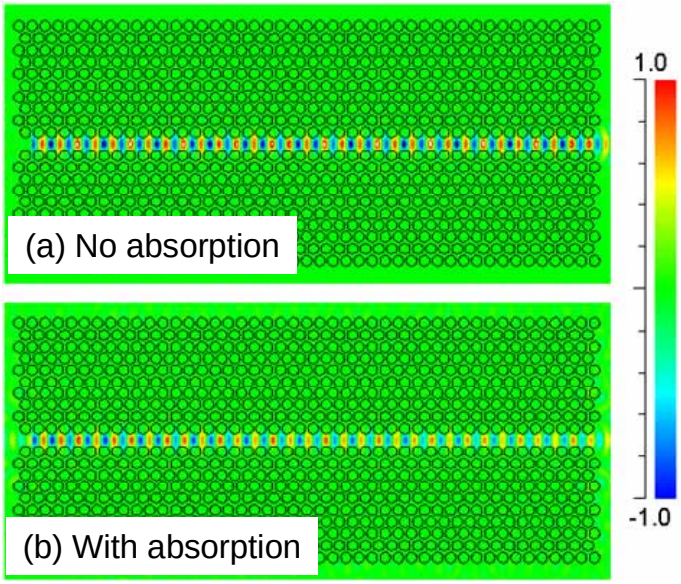

Fig. 11. The propagation field profile shown in the line-defect region is corresponding the the case shown in Table 1 for GaP/Si case with index of 2.0/3.42, r/a=0.40 and wavelength of 23.06 μm. Note the intensity difference for two cases without and with absorption.

Going into more specifics about Table 1 and Table 2, we learned that Window 2 (wavelengths *d*,*e*,*f*) is not practical due to its losses of over 1000 dB/cm. The best operation wavelengths are in Window 1 (wavelengths *a*,*b*,*c*) optimally at the short-wavelength end of the window, near point *a* in Fig. 4. In the test cases of λ = 23.06 μm or 25.58 μm for Si/GaP as well as λ = 31.27 μm or 34.50 μm for Ge/GaAs, we see that the type 2 PhC waveguides have TE loss of 125 dB/cm for GaP in Si, TM loss of 179 dB/cm for GaP in Si, TE loss of 204 dB/cm for GaAs in Ge and TM loss of 175 dB/cm for GaAs in Ge.

On the Si or Ge chip, we can seamlessly interconnect several PhC waveguide devices in an infrared "series" to form an infrared network-- an LWIR integrated circuit. In practice, the maximum useable infrared pathlength in the on-chip network, P_{max}, will be determined by the maximum infrared insertion loss L_{max} that can be "tolerated" for this photonic circuit. We have plotted P_{max} in Fig. 12 as a function of propagation loss for L_{max} of 3dB and 10 dB. Thus, referring the loss results cited in the previous paragraph, we find from Fig. 12 for the 10

#84558 - $15.00 USD Received 26 Jun 2007; revised 2 Aug 2007; accepted 3 Aug 2007; published 8 Aug 2007

dB case that P_{max} is 800 μm for GaP in Si (TE), 559 μm for GaP in Si (TM), 490 μm for GaAs in Ge (TE) and 571 μm for GaAs in Ge (TM). The paths are shorter in the 3 dB case: 240, 168, 147, and 171 μm, respectively.

Table 1. Si/GaP photonic-crystal bandgap and propagation losses: the first six examples are in Window 1; the last four are in Window 2.

Type	Filling/Substrate (n_{filled}/n_{sub})	Photonic Bandgap			λ (μm)	Without absorption		With absorption	
			TE	TM		TE	TM	TE	TM
		r/a	a/λ	a/λ		Loss dB/cm	Loss dB/cm	Loss dB/cm	Loss dB/cm
1	Si/GaP *(3.42/2.0)*	0.28	/	0.2225~0.2556	23.06	/	242	/	786
2	GaP/Si*(2.0/3.42)*	0.40	0.2296 - 0.2554	/	23.06	5.77	/	125	/
1	Si/GaP *(3.42/0.36)*	0.20	0.5567 ~ 0.5909	0.2867 ~ 0.5289	25.58	1.01	/	/	/
2	GaP/Si *(0.36/3.42)*	0.44	0.3037 ~ 0.6695	0.3968 ~ 0.4545	25.58	5.02	4.02	668	179
1	Si/GaP *(3.42/2.0)*	0.28	/	0.2225~0.2556	27.15	/	279	/	/
2	GaP/Si*(2.0/3.42)*	0.40	0.2296~0.2554	/	27.15	4.99	/	444	/
1	GaP/Si *(4.78/3.42)*	0.28	/	0.1539~0.1590	27.22	/	2407	/	3141
1	GaP/Si *(8.06/3.42)*	0.20	0.2823 ~ 0.3013	0.1133 ~ 0.1532	27.80	8.00	69.3	1029	/
2	Si/GaP *(3.42/8.06)*	0.40	0.1023 ~ 0.1381	0.2731 ~ 0.2761	27.80	0.09	299	/	/
1	GaP/Si *(4.78/3.42)*	0.28	/	0.1539~ 0.1590	30.00	/	300	/	3159

Table 2. Ge/GaAs photonic-crystal bandgap and propagation losses: the first six examples are in Window 1, the last four are in Window 2.

Type	Filling/Substrate (n_{filled}/n_{sub})	Photonic Bandgap			λ (μm)	Without absorption		With absorption	
			TE	TM		TE	TM	TE	TM
		r/a	a/λ	a/λ		Loss dB/cm	Loss dB/cm	Loss dB/cm	Loss dB/cm
1	Ge/GaAs *(3.989/2.5)*	0.28	/	0.1889~0.2094	31.27	/	226	/	1209
2	GaAs/Ge *(2.5/3.989)*	0.40	0.1939 ~0.2074	/	31.27	9.17	/	204	/
1	Ge/GaAs *(3.99/0.761)*	0.20	0.4609 ~0.4995	0.2433 ~0.4319	34.50	3.74	/	/	/
2	GaAs/Ge *(0.761/3.99)*	0.44	0.2551 ~0.5160	0.3395 ~0.3807	34.50	1.06	1.01	585	175
1	Ge/GaAs *(3.989/2.5)*	0.28	/	0.1889~0.2094	36.87	/	169.5	/	/
2	GaAs/Ge *(2.5/3.989)*	0.40	0.1939 ~0.2074	/	36.87	9.35	/	/	/
1	GaAs/Ge *(5.6/3.989)*	0.28	/	0.1315 ~0.1361	36.94	/	1886	/	2016
1	GaAs/Ge *(10.6/3.989)*	0.20	0.2284 ~0.2509	0.0875 ~0.1266	37.52	27.6	32.6	1832	6676
2	Ge/GaAs *(3.989/10.6)*	0.40	0.2104 ~0.2197	0.0788 ~0.1139	37.52	0.12	90.7	/	/
1	GaAs/Ge*(5.6/3.989)*	0.28	/	0.1315 ~0.1361	39.79	/	1727	/	/

#84558 - $15.00 USD Received 26 Jun 2007; revised 2 Aug 2007; accepted 3 Aug 2007; published 8 Aug 2007

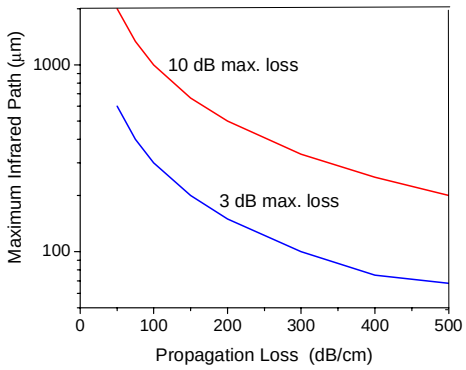

Fig. 12. Maximum infrared path *vs* attenuation for 3 dB and 10 dB total insertion loss

5. Conclusions

We have proposed and simulated a new family of 2D photonic crystals comprised of two intrinsic semiconductors, one of which undergoes a large index dispersion in the far infrared due to LO and TO phonon-absorption peaks. The lattice-matched pairs investigated here include GaAs/Ge and GaP/Si. We have also modeled a category of 2D A/B semiconductor crystal ("type 2 photonic") in which the refractive index of the slab material A is lower than the index of material B that fills the periodic array of holes within the slab. In the Reststrahl region, photonic bandgaps are found for both TE and TM modes in both type 1 and type 2 photonic crystals. Type 2 is optimal because the propagation losses for type 2 line-defect waveguides are in the 125 to 200 dB/cm range. These structures offer promise for the integration of III-V materials (GaP, GaAs) on group IV (Si, or Ge) for active far-infrared photonics, such as light sources, amplifiers, modulators, reconfigurable waveguides and switches.

Acknowledgments

The authors acknowledge the help from Dr. M. Lu and L. Chen. This work was supported in part by the U.S. Air Force Office of Scientific Research (Dr. Gernot Pomrenke).

#84558 - $15.00 USD Received 26 Jun 2007; revised 2 Aug 2007; accepted 3 Aug 2007; published 8 Aug 2007